FINITE ELEMENT METHOD ELECTRICAL IMPEDANCE TOMOGRAPHY FOR PHASE DISTRIBUTION DETERMINATION IN MULTIPHASE FLOWS: VALIDATION CALCULATIONS AND EXPERIMENTS*

J. R. Torczynski, T. J. O'Hern, and K. A. Shollenberger
Engineering Sciences Center
Sandia National Laboratories
Albuquerque, New Mexico 87185-5800

S. L. Ceccio and A. L. Tassin
Department of Mechanical Engineering and Applied Mechanics
University of Michigan
Ann Arbor, Michigan 48109-2125

ABSTRACT

A finite-element-method (FEM) implementation of electrical-impedance tomography (EIT) is described in which the spatial variation of the electrical conductivity is represented by a function with a modest number of adjustable parameters. The FEMEIT algorithm is applied to both numerical and experimental data sets generated from prescribed conductivity fields. Good agreement is found between the prescribed and reconstructed conductivity fields in both circumstances.

NOMENCLATURE

$c_1, \ldots$	=	adjustable conductivity parameters
$\mathbf{j}$	=	current flux vector (A/m^2)
J	=	current line source strength (A/m)
$\mathbf{n}$	=	outward unit normal vector (unitless)
$p_1, \ldots$	=	nonadjustable conductivity parameters
r	=	radial coordinate in conductivity function (m)
V	=	electrical potential (V)
x, y, z	=	Cartesian coordinates (m)
σ	=	electrical conductivity ($\Omega^{-1}m^{-1}$)

INTRODUCTION

The spatial variation of the gas volume fraction in bubbly flows is of importance to many industrial processes such as indirect coal liquefaction, in which a reactive gas is bubbled through a catalyst-laden liquid (slurry). More specifically, significant spatial nonuniformity in gas volume fraction can often induce large-scale buoyancy-driven recirculating flows which result in reduced process efficiency. Thus, it is important to be able to characterize the gas volume fraction spatial variation in bubbly flows.

One means by which this can be achieved is electrical-impedance tomography (EIT) (cf. Ceccio and George, 1996). Figure 1 shows a schematic diagram of an EIT setup. A region of material is surrounded by an insulating boundary on which several probes (electrodes) are mounted. A known current is injected into the material from one probe and is withdrawn from another, and voltages are measured at all probes (both current-carrying and those that carry no current). This process is repeated for different pairs of probes until all combinations of probes have been examined. When tomographic reconstruction techniques are applied, the resulting voltage and current data yield information about the spatial variation of the electrical conductivity of the medium under examination. In the case of air-water bubbly flow, the electrical conductivity is roughly proportional to the liquid volume fraction since the gas bubbles are insulating whereas the liquid is weakly conducting (see Ceccio and George (1996) for a detailed treatment of the relationship between conductivity and gas and liquid volume fractions).

The methodology, efficiency, and accuracy of various EIT tomographic reconstruction algorithms continue to be a subject of research (cf. the reviews of Hua and Woo (1990), Jones et al. (1993), and Ceccio and George (1996)). EIT algorithms can be broadly grouped in terms of the problem dimensionality (2 or 3), the impedance model employed (e.g., resistive, capacitive), the numerical method used to discretize the equations (e.g., finite element method (FEM), boundary element method (BEM)), the representation of the impedance field (e.g., piecewise constant, exponential), the means by which the impedance field is modified during an iteration (e.g., back-projection between equipotential lines, Newton-Raphson), and the intended application (e.g., biomedical imaging, multiphase flow measurement).

The purpose of the present study is not to develop a new type of algorithm or a more efficient one but rather to implement an EIT algorithm suitable for making spatially resolved measurements of

*This work was performed at Sandia National Laboratories, supported by the U. S. Department of Energy, under contract number DE-AC04-94AL85000.

gas volume fraction in gas-liquid bubbly flow. In contradistinction to the work of Lin et al. (1993), the emphasis here is not on the accurate determination of arbitrary gas-liquid interfaces or other sharp discontinuities in electrical properties. Instead, the medium under consideration (a continuum liquid phase within which a very large number of small gas bubbles are dispersed) is assumed to have smoothly varying electrical properties when averaged over length scales large compared with the bubble size and separation but small compared with the extent of the medium.

ALGORITHM AND APPLICATIONS

Following Yorkey et al. (1987), the basic EIT reconstruction algorithm is as follows (greater detail is provided in the appendix). The medium is treated as purely resistive (no capacitive contribution), which is reasonable for the air-water system considered here. The probes are treated as small in width compared with their separations so that current-bearing probes can be treated as two-dimensional point sources/sinks. The electrical conductivity is represented as an arbitrary function of position and one or more (adjustable) conductivity parameters. A finite-element method (FEM) representation of the voltage equation (formally identical to the steady heat-conduction equation with voltage and electrical conductivity replacing temperature and thermal conductivity) is formed and solved to find both the predicted voltages at probes and the derivatives of the probe voltages with respect to the conductivity parameters. A Newton-Raphson algorithm is then used to adjust the conductivity parameters to minimize the least-squares difference between the computed and experimental probe voltages. Although applied here only to two-dimensional circular geometries, the FEMEIT algorithm is general to arbitrary two-dimensional and three-dimensional geometries surrounded by an insulating boundary through which current is injected or withdrawn at discrete points.

A computer code has been written to implement this algorithm. The code treats general two-dimensional domains, including multiply connected domains and domains with internal probes. Linear triangle elements are used to construct the partial global stiffness matrices. Since probes are represented as mathematical points, a node must be placed at each probe. The conductivity functions are selected from a library of choices in a subroutine.

Three types of validation calculations have been performed. The first type involves using the analytical result for the voltage distribution with a constant conductivity σ in a circular domain in which a current J per unit length is injected at the point (x_0, y_0) and withdrawn at the point $(x_0, -y_0)$, as illustrated in Figure 1:

$$V(x,y) = \left(\frac{J}{2\pi\sigma}\right)\ln\left[\frac{(y_0+y)^2+(x_0-x)^2}{(y_0-y)^2+(x_0-x)^2}\right]$$

The radius of the circular domain, the current per unit length, and the conductivity are taken to be unity. As in O'Hern et al. (1995), 16 EIT probes are considered (see Figure 1). By proper selection of the injection and withdrawal points and by rotation of the coordinate system, the boundary voltages are determined for all possible probe pairs from the analytical solution. These boundary voltages, along with mesh information and specification of the conductivity function type, comprise the inputs to the FEMEIT code. For this study, the conductivity is taken to be an unknown constant (i.e. one unknown parameter in the minimization). Table 1 shows the dependence of the conductivity determined using this functional representation for 5 meshes of appreciably different nodal density, shown in Figure 2. In all cases, the conductivity thus determined is seen to be close to unity and appears to be converging to unity with increasing nodal density.

Table 1: Mesh refinement study for constant conductivity.

Mesh	No. Nodes	No. Elements	Computed σ
A	25	32	1.0443
B	81	128	1.0122
C	169	288	1.0047
D	289	512	1.0023
E	441	800	1.0013

The second type of validation calculation involves using the finite-element code FIDAP (Fluid Dynamics International, 1995) to compute the boundary voltages corresponding to the electrical conductivity spatial distribution shown in Figure 3. This distribution is chosen to mimic a maldistributed bubble-column flow in which an excess of bubbles is in the upper right quadrant. A highly refined mesh comprised of 9-node isoparametric quadrilaterals, shown in Figure 3, is employed to guarantee that the FIDAP solution is mesh-independent. As in the previous case, 16 EIT probes are located at integer multiples of 22.5° around the perimeter. The type of conductivity function used by the FEMEIT code is chosen to be a linear combination of the products of 15 conductivity parameters and the polynomials $\{1, x, y, x^2, xy, y^2, x^3, x^2y, xy^2, y^3, x^4, x^3y, x^2y^2, xy^3, y^4\}$. Figure 4 shows the mesh used for this simulation (identical to the E mesh of Table 1) and the reconstructed conductivity field produced by the algorithm, where FIDAP has been used to post-process the FEMEIT results. Agreement is again seen to be good.

The third type of validation calculation involves using experimentally generated data acquired with a previously reported 16-probe EIT apparatus (O'Hern et al., 1995). In brief, the apparatus employs 16 probes, mounted on the inner surface of a 7.5 in. ID lucite cylinder. The probes are 0.25 in. × 3.0 in. strips of 0.003 in. thick stainless steel. To enforce two-dimensionality for validation purposes, the bottom and top of the lucite cylinder are capped off at the probe ends with lucite end plates. A spatially varying conductivity field is established by filling the lucite cylinder with water and placing a 2.725 in. diameter PVC cylinder within the lucite cylinder at a specified location. Boundary voltages have been acquired for two positions of the PVC cylinder, one significantly eccentric and the other approximately concentric, as shown in Figure 5. These distributions are chosen to mimic two possible types of maldistribution in a bubble column:

asymmetric attachment of the gas flow to one wall and significant axisymmetric radial variation. The following form is employed in the FEMEIT code for the spatial variation of the conductivity:

$$\sigma = c_1\left\{1+\frac{p_1}{2}\left[\tanh\left(\frac{r-c_2}{p_2}\right)-\tanh\left(\frac{r+c_2}{p_2}\right)\right]\right\}$$

where $r^2 = (x-c_3)^2 + (y-c_4)^2$, $\{c_1, c_2, c_3, c_4\}$ are adjustable conductivity parameters, and $\{p_1,\ p_2\}$ are nonadjustable parameters. This function represents a circular region of radius c_2 centered at (c_3, c_4) with a boundary thickness proportional to $2p_2$, well inside of which the conductivity is approximately $c_1(1-p_1)$ and well outside of which the conductivity is approximately c_1. If p_1 is chosen close to but smaller than unity and p_2 is taken to be small compared with c_2, this function represents an insulating cylinder, where its position, radius, and external conductivity are free to vary. FEMEIT calculations are performed using the mesh of Figure 4 and the above function with the nonadjustable parameters assigned values of $1-p_1 = 0.02$ and $2p_2 = 0.1$, where the lucite cylinder has been normalized to unity radius. The calculated conductivity fields are shown in Figure 5 and agree well with the experimentally prescribed conductivity fields. No dependence on the initial values of the adjustable parameters is seen: the calculations consistently yield values of 2.72 ± 0.01 in. for the PVC cylinder diameter.

CONCLUSIONS AND FUTURE EFFORTS

A finite-element method electrical impedance tomography (FEMEIT) algorithm has been implemented and applied to perform validation calculations based on prescribed electrical conductivity fields. In all cases, the reconstructed conductivity fields agree reasonably well with the prescribed fields. Future efforts will focus on implementing this algorithm in three dimensions since ensuring two-dimensionality of both the electrical field and the bubbly flow simultaneously is problematic.

ACKNOWLEDGMENTS

This work was performed at Sandia National Laboratories, supported by the U. S. Department of Energy under contract number DE-AC04-94AL85000, through a laboratory directed research and development (LDRD) contract.

REFERENCES

Ceccio, S. L., and George, D. L., 1996, "A Review of Electrical Impedance Techniques for the Measurement of Multiphase Flows," Journal of Fluids Engineering, accepted.

Fluid Dynamics International, 1995, *FIDAP Users Manual*, Fluid Dynamics International, Evanston, IL.

Hua, P., and Woo, E. J., 1990, "Reconstruction Algorithms," *Electrical Impedance Tomography*, J. G. Webster, ed., Adam Hilger, Bristol and New York, Chapter 10.

Jones, O. C., Lin, J.-T., Ovacik, L., and Shu, H.-J., 1993, "Impedance Imaging Relative to Gas-Liquid Systems," Nuclear Engineering and Design, Vol. 141, pp. 159-176.

Lin, J.-T., Jones, O. C., Ovacik, L., and Shu, H.-J., 1993, "Advances in Impedance Imaging Relative to Two-Phase Flow," ANS Proc., Thermal Hydraulics Division, Vol. 7, pp. 68-75.

O'Hern, T. J., Torczynski, J. R., Ceccio, S. L., Tassin, A. L., Chahine, G. L., Duraiswami, R., and Sarkar, K., 1995, "Development of an Electrical Impedance Tomography System for an Air-Water Vertical Bubble Column," in *Forum on Measurement Techniques in Multiphase Flows*, FED-Vol. 233, J. W. Hoyt, T. J. O'Hern, C. Presser, A. K. Gupta, and R. L. Alpert eds., American Society of Mechanical Engineers, New York, pp. 531-537.

Yorkey, T. J., Webster, J. G., and Tompkins, W. J., 1987, "Comparing Reconstruction Algorithms for Electrical Impedance Tomography," IEEE Transactions on Biomedical Engineering, Vol. BME-34, No. 11, pp. 843-852.

APPENDIX

The voltage field V is normalized by the injection current J per unit length and is represented as $v = \Sigma_j v_j \phi_j(x,y)$, where the ϕ_j are the finite-element shape functions. The conductivity field is represented as $\sigma = \sigma(x, y; \{\sigma_\beta\})$, where the σ_β are adjustable conductivity parameters. The experiment with current injected at node m and withdrawn from node n is denoted by (mn). The equation is $\nabla \cdot \sigma \nabla v^{(mn)} = 0$, and the boundary condition for each experiment is $\sigma \mathbf{n} \cdot \nabla v^{(mn)} = \delta(s - s^{(m)}) - \delta(s - s^{(n)})$, where s is the arc length along the boundary with probes m and n at $s^{(m)}$ and $s^{(n)}$, respectively. The conductivity parameters are adjusted until the following quantity is minimized:

$$\Gamma = \frac{1}{2}\sum_k \sum_{(mn)} w_k^{(mn)}\left(v_k^{(mn)} + \sum_\beta \frac{\partial v_k^{(mn)}}{\partial \sigma_\beta}\delta\sigma_\beta + v_0^{(mn)} - \tilde{v}_k^{(mn)}\right)^2$$

Here, k is the probe node number, $v_0^{(mn)}$ are the voltage offsets (additional adjustable parameters), $\tilde{v}_k^{(mn)}$ are the experimentally measured normalized voltages, $\delta\sigma_\beta$ are the updates to the conductivity parameters, and $w_k^{(mn)}$ is 0 if $k = m$ or $k = n$ but is 1 otherwise. The following steps are taken to minimize Γ.

1. Assemble the stiffness and Jacobian matrices M_{ij} and $P_{\alpha ij}$: $M_{ij} = \int \sigma \nabla\phi_i \cdot \nabla\phi_j da$, $P_{\alpha ij} = \int (\partial\sigma/\partial\sigma_\alpha)\nabla\phi_i \cdot \nabla\phi_j da$
2. Find all values $W_{jk} = W_{kj}$ given by $\Sigma_j M_{ij} W_{jk} = \delta_{ik}$, where k is a probe node number and i and j are any node numbers.
3. Find the normalized voltages $v_k^{(mn)} = v_k^{(m)} - v_k^{(n)}$ at the probe nodes k where $v_k^{(m)} = W_{km}$.
4. Find the normalized voltage derivatives at the probe nodes k:

$$\frac{\partial v_k^{(mn)}}{\partial \sigma_\alpha} = \frac{\partial v_k^{(m)}}{\partial \sigma_\alpha} - \frac{\partial v_k^{(n)}}{\partial \sigma_\alpha} \quad \text{where} \quad \frac{\partial v_k^{(m)}}{\partial \sigma_\alpha} = -\sum_{i,j} W_{ki} P_{\alpha ij} W_{jm}$$

5. Form $A_{\alpha\beta}$ and B_α:

$$A_{\alpha\beta} = \sum_{k,l}\sum_{(mn)} w_k^{(mn)} w_l^{(mn)}\left(\frac{\partial v_k^{(mn)}}{\partial \sigma_\alpha} - \frac{\partial v_l^{(mn)}}{\partial \sigma_\alpha}\right)\frac{\partial v_k^{(mn)}}{\partial \sigma_\beta}$$

$$B_\alpha = \sum_{k,l}\sum_{(mn)} w_k^{(mn)} w_l^{(mn)}\left(\frac{\partial v_k^{(mn)}}{\partial \sigma_\alpha} - \frac{\partial v_l^{(mn)}}{\partial \sigma_\alpha}\right)\left(\tilde{v}_k^{(mn)} - v_k^{(mn)}\right)$$

6. Solve $\Sigma_\beta A_{\alpha\beta}\delta\sigma_\beta = B_\alpha$ and update $\sigma_\beta \to \sigma_\beta + \delta\sigma_\beta$.

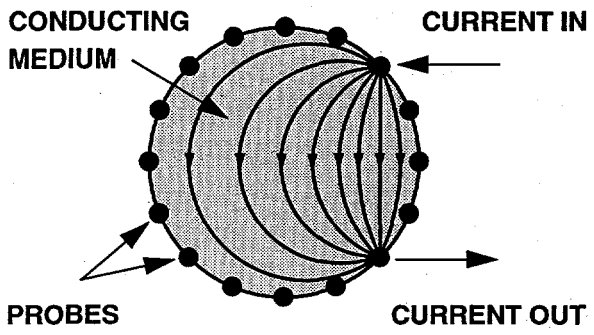

Figure 1. Schematic diagram of an EIT setup with 16 probes.

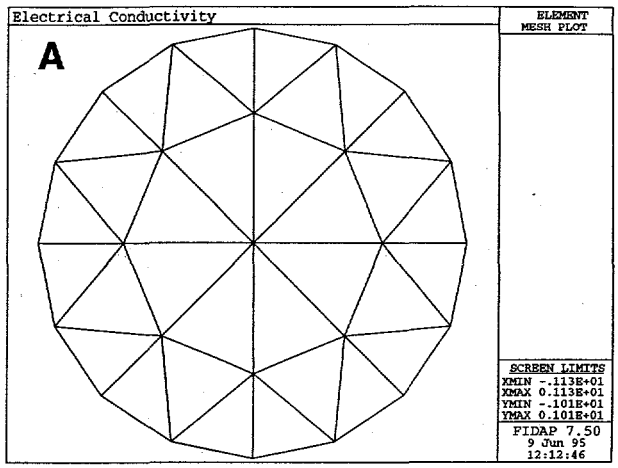

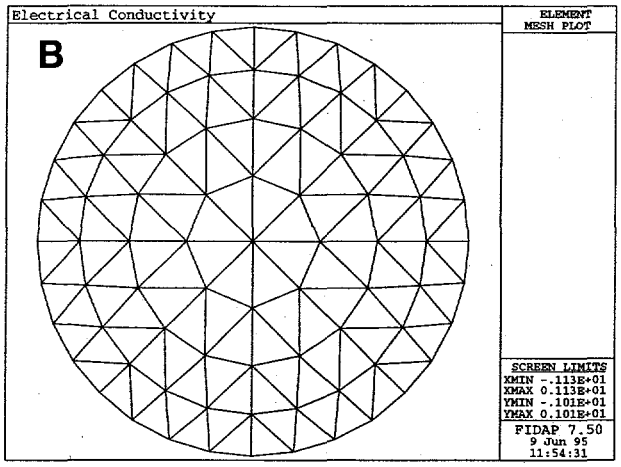

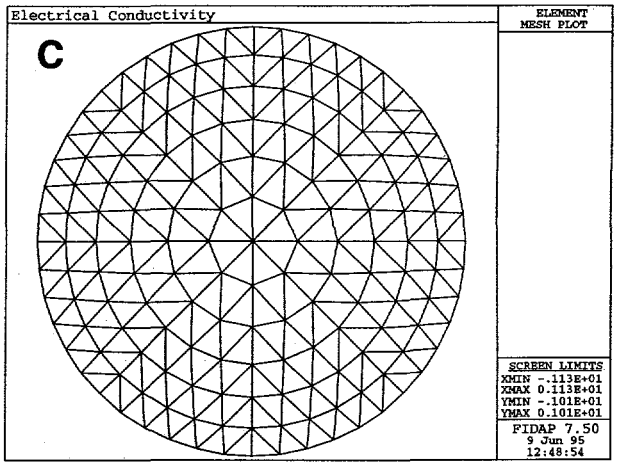

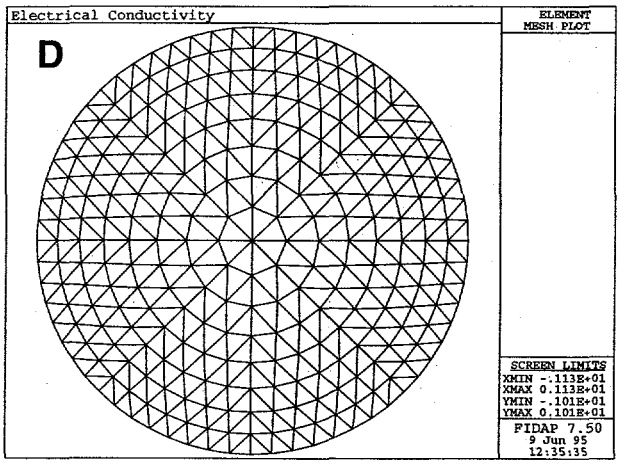

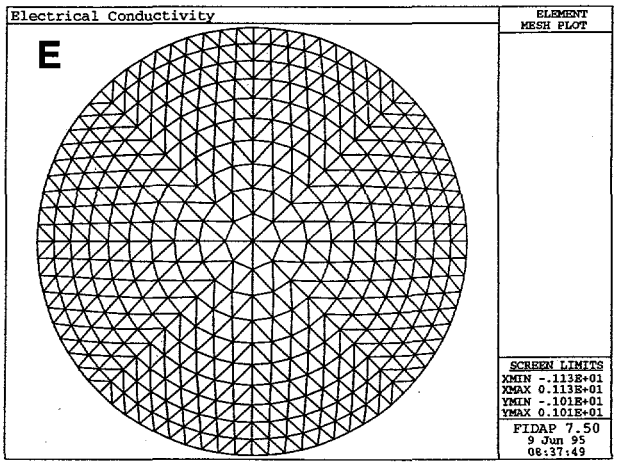

Figure 2. Meshes for constant-conductivity study: A (top right), B (middle left), C (middle right), D (bottom left), E (bottom right).

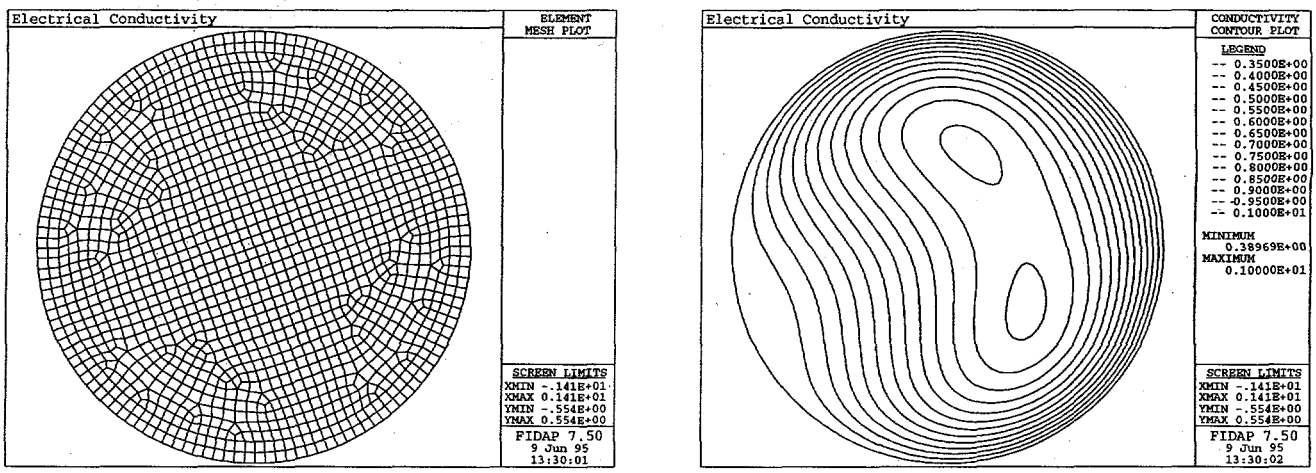

Figure 3. Left, FIDAP mesh (9-node isoparametric quadrilaterals); right, prescribed electrical conductivity field used to generate "numerical" EIT data. Boundary voltages calculated by FIDAP using this electrical conductivity field are inputs to FEMEIT.

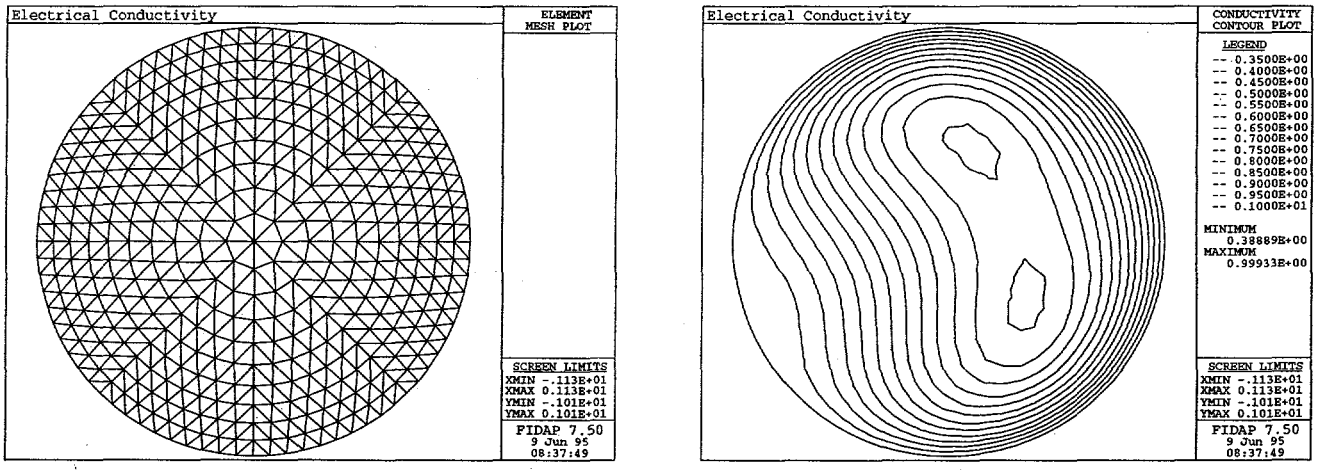

Figure 4. Left, FEMEIT mesh (linear triangles, the E mesh of Table 1); right, reconstructed electrical conductivity field based on numerically generated EIT data. Good agreement is seen with the previous figure.

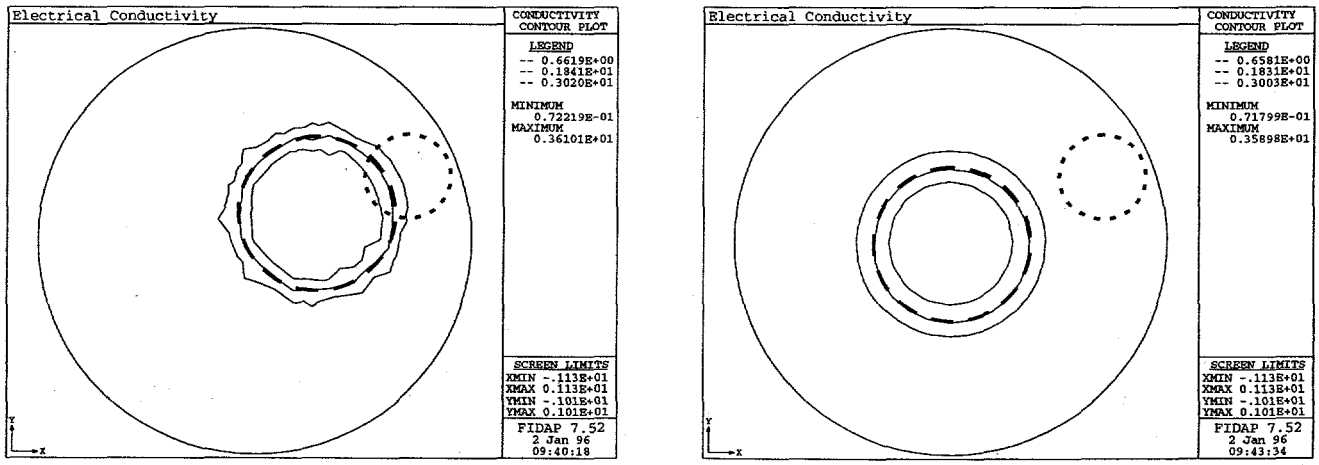

Figure 5. Reconstructions of a PVC (insulating) cylinder using the E mesh: left, eccentric placement; right, concentric placement. The long-dashed curves show the placement and size of the cylinder, and the short-dashed curves show the initial guess of its placement and size.

DISCLAIMER